A New Cytotoxic Steroidal Glycoalkaloid from the Methanol Extract of *Blumea lacera* Leaves

Raushanara Akter[1, 2], Shaikh J. Uddin[1,3], Joe Tiralongo[4], I. Darren Grice[4,5], Evelin Tiralongo[1,6]

[1] School of Pharmacy, Griffith University, Gold Coast campus, Queensland, Australia. [2] Department of Pharmacy, BRAC University, Dhaka, Bangladesh. [3] Pharmacy Discipline, Khulna University, Khulna, Bangladesh. [4] Institute for Glycomics, Griffith University, Gold Coast campus, Queensland, Australia. [5] School of Medical Science, Griffith University, Gold Coast campus, Queensland, Australia. [6] Menzies Health Institute Queensland, Griffith University, Gold Coast campus, Queensland, Australia.

Received, July 13, 2015; Revised, September 14, 2015; Accepted, October 7, 2015; Published, October 18, 2015.

ABSTRACT – PURPOSE: *Blumea lacera* (*B. lacera*) (Asteraceae) is a well-known Bangladeshi medicinal plant. This study aimed to identify and characterize constituents associated with the significant cytotoxic activity of this plant that we reported previously. Here, we describe the isolation and characterization of a new steroidal glycoalkaloid (SGA) **1**, the evaluation of its cytotoxic activity, apoptotic potential, and effect on cell cycle in comparison to analogous steroidal glycoalkaloids (SGAs). **METHODS:** SGA **1** was isolated using C_{18} SPE and HPLC, and subsequently structurally characterized using 1D and 2D NMR, MS and other spectroscopic methods, along with a comparative inspection of the literature. Cytotoxic activity of **1** and seven SGA analogues and steroidal alkaloids (SAs), (β-solamarine, α-solanine, β-solamargine, α-solasonine, khasianine, solasodine, tomatidine HCl) were evaluated for their cytotoxicity against two healthy (NIH3T3 and VERO) and four human cancer (AGS, HT-29, MCF-7 and MDA-MB-231) cell lines using the MTT assay. Cytotoxic SGAs were further evaluated for apoptosis-inducing potential and cell cycle arresting ability against breast cancer cells (MCF-7) using the FITC Annexin V and propidium iodide (PI) assay. **RESULTS:** Bioactivity guided fractionation of the methanol extract of *B. lacera* led to isolation of compound **1:** (25*R*)-3β-{*O*-β-D-glucopyranosyl-(1→4)-*O*-α-L-rhamnopyranosyl-(1→4)-[*O*-α-L-rhamnopyranosyl-(1→2)]-α-L-rhamnopyranosyl}-22αN-spirosol-5-ene. SGA **1** was the most cytotoxic compound against a number of human cancer cell lines with an IC_{50} of 2.62 μM against MCF-7 cells. It displayed the highest apoptotic potential (32% AV^+/PI^-) on MCF-7 cells compared to other cytotoxic SGA analogues and a slight, but significant cell cycle arresting effect. **CONCLUSIONS:** A new SGA **1** was isolated from *B. lacera* and its cytotoxic activity, as well as that of other SAGs, was evaluated. SAR investigations on SGA **1**, in relation to SGA analogues, show that the number and nature of sugar moieties along with the linkages of the sugar to the aglycone are crucial for cytotoxic and apoptotic activity.

INTRODUCTION

Blumea lacera (Burn. f.) DC. (Asteraceae) is a herbaceous weed locally known as Kukursunga in Bangladesh (1). It is also commonly found in India, Australia, China, Malaya and tropical Africa (2). The plant is used traditionally as an anthelmintic, astringent, diuretic, anti-scorbutic, anti-dysentric, antimicrobial, anti-inflammatory and carminative agent, as well as for the treatment of cholera and catarrhal infections (3, 4). It is reported to cure bronchitis, blood diseases and fevers, and to alleviate burning sensations (2). The hot water extract of *B. lacera* has been reported to have anti-leukemic activity against anti-K562, L1210, P3HR1, Raji and U937 leukemia cells (5). Recently, we reported on the cytotoxic activity of methanolic and water extracts of *B. lacera* against a number of human cancer cell lines (6). Phytochemical studies of the plant have thus far reported the isolation of a total of 17 compounds belonging to natural product classes such as flavonoids, terpene glycosides, phenol glycosides,

Corresponding Author: Associate Professor Evelin Tiralongo, School of Pharmacy, Griffith University, Gold Coast campus, Queensland, Australia, E-mail address: e.tiralongo@griffith.edu.au.

essential oils, coniferyl alcohol derivatives and terpenoid ketones (2, 3, 7-12). Antibacterial and antifungal activities of the monoterpene glycosides isolated from this plant have also been previously reported (4). However, there are no reports to date that have attributed the cytotoxic activity, observed in extracts of *B. lacera,* to specific compounds. Moreover, so far only the phytosterol campesterol has been identified from this plant (13).

This study reports on a new SGA **1**, namely (25*R*)-3β-{*O*-β-D-glucopyranosyl-(1→4)-*O*-α-L-rhamnopyranosyl-(1→4)-[*O*-α-L-rhamnopyranosyl-(1→2)]-α-L-rhamnopyranosyl}-22αN-spirosol-5-ene isolated and characterized from the methanolic extract of *B. lacera* leaves. SGAs are comprised of an aglycone and a sugar moiety, with both the aglycone and sugar moieties impacting on the compound's bioactivity, including their cytotoxic and anticancer activity (14-17). For some SGAs, but not all, the structure-activity relationship (SAR) regarding their cytotoxic activity has been reported (14-17).

In this study, the new SGA **1**, as well as seven structurally similar SGAs and SAs (β-solamarine, α-solanine, β-solamargine, α-solasonine, khasianine, solasodine, tomatidine HCl) were evaluated for cytotoxicity against two healthy (NIH3T3 and VERO) and four human cancer (AGS, HT-29, MCF-7 and MDA-MB-231) cell lines using the MTT assay. In addition, apoptosis and cell cycle studies were performed for compound **1** and the cytotoxic SGAs (many of which had previously not been evaluated in this way) to identify the mechanism of cytotoxic activity, determine SARs and evaluate these compounds for their potential in anticancer therapy.

METHODS

General experimental procedures

Optical rotation was measured on a JASCO P-1010 polarimeter. The UV and IR spectra were recorded on a Shimadzu BioSpec-mini and a Bruker Optics alpha-QuickSnap (A220/D-01) spectrophotometer, respectively. NMR spectra (^{1}H NMR, ^{13}C NMR, ^{1}H-^{1}H COSY, HSQC and HMBC) were recorded on either a Bruker Avance 300 or 600 MHz spectrometer in CD_3OD with TMS as an internal standard. The chemical shifts (δ) are expressed in ppm and the coupling constants (*J*) are in Hz. The mass spectra (LRMS and HRESIMS) were recorded on a Bruker Daltonics Esquire 3000 and Bruker Daltonics Apex III 4.7e spectrometers, respectively. Analytical HPLC was performed on a Varian Prostar instrument with a 335 DAD using a RP (Luna C_{18}, 5 μm, 250 × 4.6 mm) column. Preparative HPLC was performed on a Waters instrument equipped with a Waters 600E pump, Rheodyne 7725i injector, and Waters 2487 dual-wavelength detector using a RP (Luna C18, 5 μm, 150 x 21.2 mm) column. SPE cartridges (Alltech, 10 g, RP-C18) were used to fractionate the extract.

Plant material

The leaves of *B. lacera* were collected from the Southern part of Bangladesh in May 2007. A voucher specimen of *B. lacera* (No. DACB 30550) was identified by Dr. Momtaz Mahal Mirza, Principal Scientific Officer, Bangladesh National Herbarium, Dhaka and was deposited in the Bangladesh National Herbarium, Dhaka.

Extraction and isolation

The dried and pulverised plant material of *B. lacera* (51.0 g) was extracted by soaking in 500 mL of distilled methanol overnight at room temperature with continuous stirring. The extract was then filtered and the solvent evaporated using a rotary evaporator followed by freeze-drying to afford 7.86 g (15.4 % w/w) of crude methanol extract. The extract was further fractionated using a C_{18} SPE column and eluted with a methanol/water stepwise gradient (0-100% MeOH in H_2O) to provide six SPE fractions. Cytotoxicity assays (MTT) on each of the SPE fractions was performed and the active fraction SPE5 was further subjected to purification using semi-preparative RP-HPLC (Luna 5 μm, 150 x 21.2 mm) using a H_2O/ACN gradient system containing 0.05% TFA. Semi-preparative HPLC of SPE5 (0.5 g) afforded the new SGA **1** (114.1 mg).

Cell culture and chemicals

All cell lines (VERO, ATCC: CCL-81; NIH 3T3, ATCC: CRL-1658; AGS, ATCC: CRL-1739; HT-29, ATCC: HTB-38; MCF-7, ATCC: HTB-22; and MDA-MB-231, ATCC: HTB-26) were purchased from ATCC, Manassas, VA 20108, USA. Cell lines were cultured in Advanced Dulbecco's modified Eagle's medium supplemented with 10% inactivated newborn calf serum and 5 mM l-glutamine, and grown at 37°C in a humidified atmosphere of 5% CO_2 in air. DMSO, MTT, cycloheximide and paclitaxel were purchased from Sigma Aldrich, Germany. Annexin V-FITC and

propidium iodide were purchased from BD Biosciences, NJ, USA.

Cytotoxicity assay (MTT)

In vitro cytotoxicity of the isolated SGA **1** was tested against normal mouse fibroblast (NIH3T3) and monkey kidney (VERO) cells, as well as four human cancer cell lines (gastric adenocarcinoma (AGS), colon adenocarcinoma (HT-29), and two breast ductal carcinoma cell lines (MCF-7: estrogen dependent and MDA-MB-231: estrogen non-dependent), using the MTT assay. Briefly, cells were seeded in 96-well plates at a density of 1.0 × 10^4 to 2.0 × 10^4 cells/well. Following 24 h incubation at 37°C with 5% CO_2, cells were treated with varying concentrations of SGAs and SAs for 48 h. Following washing and incubation with MTT solution for 2 h, cells were lysed. The absorbance was measured after 45 min using a microplate reader (Wallac 1420 Multilevel counter, Perkin-Elmer) at a wavelength of 560 nm. The IC_{50} values were calculated with probit analysis software (LdP Line Software, Doki, Cairo). Cycloheximide was used as a positive control, generating IC_{50} values of 8.53, 11.02, 22.39, 24.45, 26.44 and 181.87 µM against AGS, HT29, MDA-MB-231, VERO, NIH3T3 and MCF-7 cells, respectively.

Apoptosis assay

The annexin V-FITC apoptosis assay was used to measure apoptosis of the isolated cytotoxic SGA **1** from *B. lacera* against a human breast cancer MCF-7 cell line. Briefly, cells were seeded in a 6-well plate at a density of 50 × 10^4 cells/well and incubated at 37°C with 5% CO_2 for 24 h. The following day, cells were treated with IC_{50} concentrations of **1** and other SGAs for 24 and 48 h. Cells were rinsed with PBS, trypsinized rapidly, and centrifuged to pellet the cells. The supernatant was removed, and the cells were resuspended in 1× binding buffer (0.1 M Hepes/NaOH, 1.4 M NaCl, 25 mM $CaCl_2$), and 5 µL aliquots of the staining solutions (FITC annexin V and PI) were added. After 15 min incubation in the dark at room temperature, the cell suspension was diluted with binding buffer and analyzed within 1 h using a CyAn ™ ADP flow cytometer (Beckman Coulter, USA) with data recorded using HyperCyt (R) software. The assay was carried out as two separate experiments and each experiment performed in triplicate. Cells with no treatment served as the negative control and paclitaxel (0.023 µM) served as the positive control.

Cell cycle analysis

Propidium iodide staining cell cycle analysis was used to measure the cell distribution in 3 different phases of the cell cycle after treatment with **1** against breast carcinoma cells (MCF-7)). Briefly, for cell cycle analysis using flow cytometry, 15 x 10^4 cells/well were seeded in 12-well plates and incubated at 37°C with 5% CO_2 for 24 h. Following attachment of the cells after 24 h, the cells were treated with **1** and other SGAs at their IC_{50} concentrations for 24 h, after which the cells were harvested by trypsinization, washed with PBS and fixed with 70% ice cold ethanol. After 15 minutes incubation and following centrifugation, the fixed cells were incubated with 250 µL RNase A solution (0.2 mg/mL RNase and 10% Triton X-100) in PBS and incubated for 40 minutes at 37°C. The cell suspension was then transferred to a falcon polystyrene U bottom tube (5 mL) and re-suspended with 10 µL (1 mg/mL) of propidium iodide. Cell cycle distribution was analysed using a CyAn™ ADP flow cytometer (Beckman Coulter, USA) and the data recorded using HyperCyt (R) software. The results were analyzed using De novo FCS express 4 Flow Cytometry software. Cells with no treatment served as the negative control and paclitaxel (0.023 µM) served as the positive control.

RESULTS

Isolation and structural characterisation of the new SGA 1

SGA **1** was isolated and purified from the methanol extract of *B. lacera* leaves using C_{18} SPE and HPLC. The structure of **1** was elucidated by 1D and 2D NMR, MS and other spectroscopic methods. Isolated **1** was obtained as a white amorphous powder. Positive-ion mode HR-ESI-MS generated a quasi-molecular ion $[M+H]^+$ at *m/z* 1014.5616, consistent with the molecular formula $C_{51}H_{84}NO_{19}$. The measured optical rotation of the compound was $[\alpha]^{25}_D$ = -94.4° (MeOH). The UV spectrum displayed λ_{max} at 238 and 202 nm, while the IR spectrum showed major absorption bands at cm^{-1}: 3380 (OH or NH), 2934 (C-H), 1669 cm^{-1} (C=C), 1200-1000 cm^{-1} (C-O). Table 1 presents the ^1H and ^{13}C NMR spectroscopic data.

Table 1. ^{1}H and ^{13}C NMR chemical shifts for SGA **1** (CD_3OD, 300 and 75 MHz, respectively).

Position	δ_H (ppm) (multiplicity, *J*, Hz)	δ_C (ppm)
Aglycone		
1	1.85, 1.05 (2 x *m*, 2H)	38.4
2	1.89 (*m*, 2H)	30.7
3	3.55 (*m*, 1H)	79.5
4	2.27, 2.46 (2 x *m*, 2H)	39.4
5		141.8
6	5.39 (*br s*, 1H, *J*=4.5)	122.5
7	2.06, 1.98 (2 x *m*, 2H)	33.0
8	1.69 (*m*,1H)	32.7
9	0.97 (*d*, 1H, *J*=6.3)	51.5
10		38.0
11	1.58 (*m*, 2H)	21.9
12	1.79, 1.83 (2 x *m*, 2H)	40.3
13		42.1
14	2.11 (*m*, 1H)	57.6
15	1.85, 1.89 (2 x m, 2H)	33.2
16	4.63 (*dd*, 1H, *J*=7.5, 7.5)	84.7
17	1.91 (*m*, 1H)	62.9
18	0.86 (*s*, 3H)	16.5
19	1.05 (*s*, 3H)	19.8
20	2.34 (*m*, 1H, *J*=7.5)	42.8
21	1.15 (*d*, 3H, *J*=7.2)	14.7
22		100.2
23	1.85, 1.89 (2 x *m*, 2H)	33.1
24	1.71- 1.77 (*m*, 2H)	28.9
25	1.88 (*m*, 1H)	29.3
26	2.88, 3.06 (2 x *m*, 2H)	46.7
27	0.97 (*d*, 3H, *J*=6.3)	18.6
Sugar Residues		
Glc		
1	4.50 (*d*, 1H, *J*=7.8)	100.4
2	3.55 (*m,* 1H)	80.8
3	4.35 (*m,* 1H)	76.6
4	3.56 (*m,* 1H)	77.9
5	3.59 (*m,* 1H)	79.1
6a, 6b	3.65, 3.80 (2 x *m,* 2H)	61.9
Rha1		
1	5.19 (*d*, 1H, *J*=2.1)	102.3
2	3.93 (*m,* 1H)	72.3
3	3.79 (*m,* 1H)	72.8
4	3.40 (*m,* 1H)	73.8
5	4.11 (*m,* 1H)	69.7
6 ($-CH_3$)	1.24 (*d*, 3H, *J*=6.3)	17.9
Rha2		
1	5.18 (*d*, 1H, *J*=1.8)	103.1
2	3.59 (*m,* 1H)	72.3
3	4.04 (*m,* 1H)	69.0
4	3.74 (*m,* 1H)	72.9
5	3.93 (*m,* 1H)	72.1
6 ($-CH_3$)	1.25 (*d*, 3H, *J*=6.3)	18.0
Rha3		
1	4.83 (*d*, 1H, *J*=1.2)	102.6
2	3.64 (*m,* 1H)	72.3
3	3.41 (*m,* 1H)	72.3
4	3.66 (*m,* 1H)	73.9
5	3.70 (*m,* 1H)	70.4

Table 1. Continued…..

6 (-CH_3)	1.28 (*d*, 3H, *J*=6.0)	18.6

Glc = β-D-Glucopyranose, **Rha** = α-L-Rhamnopyranose

Cytotoxicity of the isolated new SGA 1 and structurally related SGA analogues

In this study, the isolated SGA **1** was evaluated for its cytotoxic activity against two healthy (NIH3T3 and VERO) and four human cancer (AGS, HT-29, MCF-7 and MDA-MB-231) cell lines using the MTT assay. Its cytotoxicity was compared to the cytotoxicity determined for seven other known and structurally related SGAs and SA derivatives, namely β-solamarine, α-solanine, β-solamargine, α-solasonine, khasianine, solasodine, tomatidine HCl. Table 2 presents the cytotoxicity results (IC_{50} values) of all SGAs tested. Overall, SGA **1** possesses relatively high cytotoxicity against all the cell lines tested (IC_{50} range 2.6-24 μM), with the lowest IC_{50} value of 2.62 μM against MCF-7 cells. Among the known SGAs and SAs tested, β-solamarine was the most cytotoxic (IC_{50} range 4.1-26 μM) with an overall similar activity to that observed for SGA **1**. The cytotoxic activity of β-solamarine against MCF-7 cells (IC_{50} 4.1 μM) was similar to that observed for SGA **1** but the cytotoxicity against the two healthy cell lines tested was higher. In addition, khasianine showed weak cytotoxic activity only against MCF-7 cells (19.89 μM). Of note, tomatidine HCl and solasodine showed no toxicity against any of the cell lines tested.

Apoptosis assay of the isolated new SGA 1 and selected SGA analogues

To determine whether SGA **1** induces apoptosis, and to compare its apoptosis-inducing potential to other SGA analogues identified as being cytotoxic (β-solamargine, β-solamarine, α-solasonine and α-solanine), annexin V-FITC apoptosis tests (24 h) against MCF-7 cells at their IC_{50} concentrations were conducted. Of all the SGAs tested the new SGA **1** showed the highest apoptotic (AV^+/PI^-) effect (32%) that was significantly above untreated cells (7.6%) (Figure 1). Amongst the known SGA analogues tested, only α-solanine and β-solamargine exhibited apoptosis-inducing potential with 22% (AV^+/PI^-) and 21% (AV^+/PI^-), respectively (Figure 1).

Cell cycle analysis of the isolated new SGA 1 and selected SGA analogues

To further explore the mechanism by which SGA **1** and other SGA analogues elicit their cytotoxicity on MCF-7 cells, cell cycle analysis using propidium iodide (PI) staining was performed. Figure 2 shows that cells treated with α-solanine displayed a significant increase in the percentage of MCF-7 cells arrested in S phase (18%), with a corresponding decrease in the percentage of cells in the G1 (57.8%) and G2/M phases (17%), compared to untreated cells (G1 phase: 62.8%, S phase: 6.3% and G2/M phase 23.2%).

Table 2. Cytotoxic activity (IC_{50}) of the isolated new SGA **1** and other known SGA analogues.

Compound	**Cytotoxic activity (IC_{50})* (μM)**					
	VERO P35	NIH3T3	AGS	HT-29	MCF-7	MDA-MB-231
SGA **1**	24.03	22.33	11.20	10.83	2.62	13.72
α-Solasodine	>100	>100	>100	>100	>100	>100
α-Solasonine	16.65	11.18	94.32	>100	5.09	8.36
β-Solamargine	53.94	47.60	21.19	16.36	5.01	20.68
Khasianine	>100	>100	>100	>100	19.89	>100
β-Solamarine	8.32	5.08	26.08	15.90	4.10	2.55
α-Solanine	42.39	44.66	31.56	22.39	4.57	6.94
Tomatidine HCl	>100	>100	>100	>100	>100	>100
Cycloheximide	24.45	26.44	8.53	11.02	181.87	22.39

IC_{50}* (Inhibition of cell growth by 50%) calculated by probit analysis (LdP Line software, USA), data was generated by two experiments performed in triplicates.

On the other hand, SGA **1**, β-solamargine, β-solamarine and α-solasonine showed similar arresting potentials, and in the case of SGA **1** significant arrest of MCF-7 cells in the G1 phase with a corresponding decrease in the percentage of cells in the G2/M (no change in cells in S phase was observed) (Figure 2). Paclitaxel, the positive control, showed a significant increase in the percentage of cells in the G2/M phase, which correlates with a decrease in the percentage of cells at the G1 phase relative to no treatment, indicating that paclitaxel induced G2/M cell cycle arrest.

DISCUSSION

Recently we reported on the cytotoxic activity of the methanolic and water extracts of *B. lacera* leaves against a number of human cancer cell lines (6). However, there are no reports to date on the isolation of cytotoxic compounds from this plant. In this study, a new SGA 1 was isolated as a white powder from the methanolic extract of *B. lacera* using SPE and HPLC. The ^{1}H NMR data (Table 1, Figure S1) of the SGA 1 evidenced a SGA structure following close examination of a reported SGA (18). Evidencing 16 oxymethine and one oxymethylene proton signals indicating the presence of three rhamnopyranose and one glucopyranose units in the glycone moiety. The ^{1}H NMR spectrum evidenced four anomeric sugar residue signals at δ_H 4.50 (*d*, 1H, *J* = 7.8 Hz), 4.83 (*d*, 1H, *J* = 1.2 Hz), 5.18 (*d*, 1H, *J* = 1.8 Hz) and 5.19 (*d*, 1H, *J* = 2.1 Hz) indicating one β-configured (*J* = 7.8 Hz) and three α-configured (*J* = 1.2, 1.8 and 2.1 Hz) sugars, respectively. One oxymethine proton signal at δ_H 4.59 ppm was attributed to ring-E of the aglycone. The remaining ^{1}H NMR signals were consistent with a SGA structure.

The ^{13}C NMR data (Table 1, Figure S2) of SGA **1** revealed the presence of fifty one different carbon signals, among which twenty seven carbon signals were attributed to the aglycone and the remaining twenty four consistent with the presence of four hexoses. The sixteen oxymethine carbon signals between δ_C 69.0-80.8 ppm and one oxymethylene proton signal at δ_C 61.9 ppm were attributed to three α-rhamnopyranose and one β-glucopyranose units. Consistent with this four anomeric carbon signals at 100.4 (Glc C-1), 102.3 (Rha1 C-1), 102.6 (Rha3 C-1), and 103.1 (Rha2 C-1) ppm were also evident, indicating again the presence of four sugar moieties; one oxymethine carbon signal at δ_C 84.7 (C-16) ppm was attributed to ring-E of the aglycone. The configuration at C-22 was determined as 22-α-N on the basis of carbon shifts at C-23, C-24 and C-26 in comparison to published ^{13}C NMR data (19, 20). The presence of the 25*R* spiroketal moiety and an axial H-25, and equatorial configuration of the methyl at C-27 was established from ^{1}H and ^{13}C NMR shifts along with comparisons to published data (21). The glycosidic linkage was shown to be at C-3 of the aglycone, due to the downfield shift of C-3 at 79.5 ppm of the glycoside when compared with the free aglycone (21).

The HMBC experiment data for SGA **1** along with the literature comparison confirmed the connectivity between ring-C-ring-D, ring-A-ring-B and ring-D-ring-C as well as ring-D-ring-E. The methine proton at δ_H 3.55 (H-3) showed connectivity to the anomeric sugar carbon at δ_C 100.4 ppm (Glc C-1) indicating the β-Glc C-1 to be C-3 linked to the aglycone of SGA **1**. In addition, connectivity of the proton at δ_H 3.55 (Glc H-2) to the carbon at δ_C 102.3 (Rha1 C-1) ppm, indicated the α-Rha1 C-1 was linked to β-Glc C-2. Cross-peaks between δ_H 3.56 (Glc H-4) and δ_C 103.2 (Rha2 C-1) ppm indicated the α-Rha2 C-1 was linked to β-Glc C-4, while cross peaks between δ_H 3.74 (Rha2 H-4) and δ_C 102.6 (α-Rha3 C-1) ppm indicated the Rha3 C-1 was linked to Rha2 C-4 (Figure 3).

Based on all NMR spectral data for SGA **1** as well as comparing with previously published SGA data the aglycone moiety of SGA **1** was assigned as (3β, 22α, 25*R*)-spirosol-5-ene (18-21) and therefore, the structure of the isolated compound **1** was assigned as a new SGA, namely (25*R*)-3β-{*O*-β-D-glucopyranosyl-(1→4)-*O*-α-L-rhamnopyranosyl-(1→4)-[*O*-α-L-rhamnopyranosyl-(1→2)]-α-L-rhamnopyranosyl}-22αN-spirosol-5-ene (Figure 4).

More than 100 structurally different SGAs belonging to solanidane and spirosolane classes have been identified to date in over 350 *Solanum* species (22, 23). SGAs are comprised of two main subunits; an aglycone unit and the glycosidic moieties. These compounds possess a wide range of bioactivities such as antifungal, anti-inflammatory, cytotoxic, antiviral, antioxidant and antimicrobial effects. Studies indicate that both, the aglycone and glycosidic moieties play crucial roles in exerting biological effects, including cytotoxic effects (24-26).

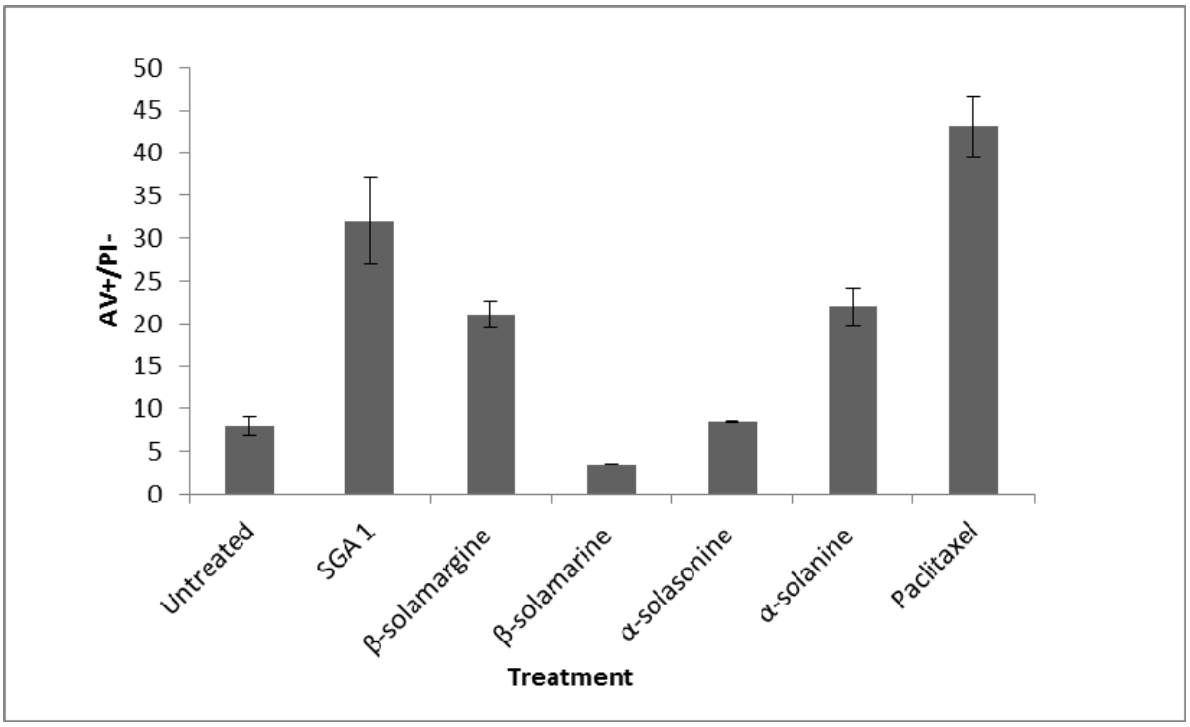

Figure 1. Apoptosis induction (AV^+/PI^-) of SGA **1** and other SGA analogues in MCF-7 cells after 24 h treatment where paclitaxel was used as a positive control.

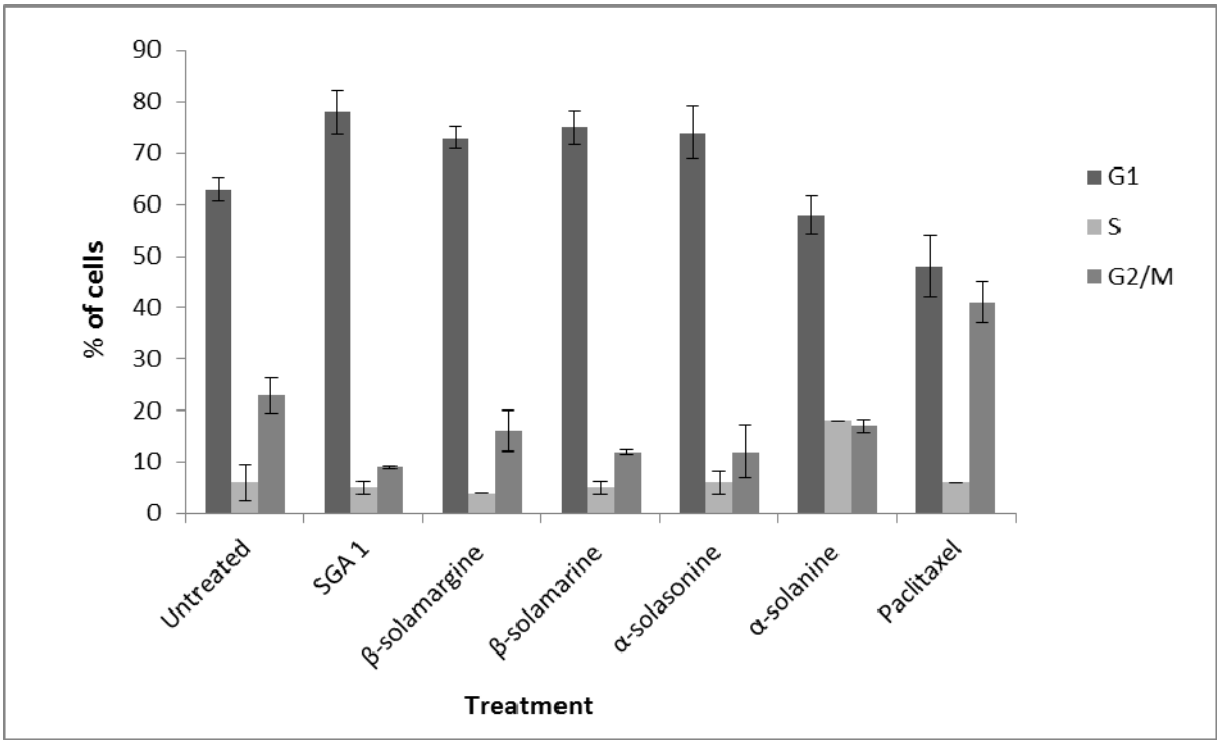

Figure 2. Cell cycle arresting potential of SGA **1** and other SGA analogues on MCF-7 cells following 24 h treatment, where paclitaxel was used as a positive control (0.023 μM).

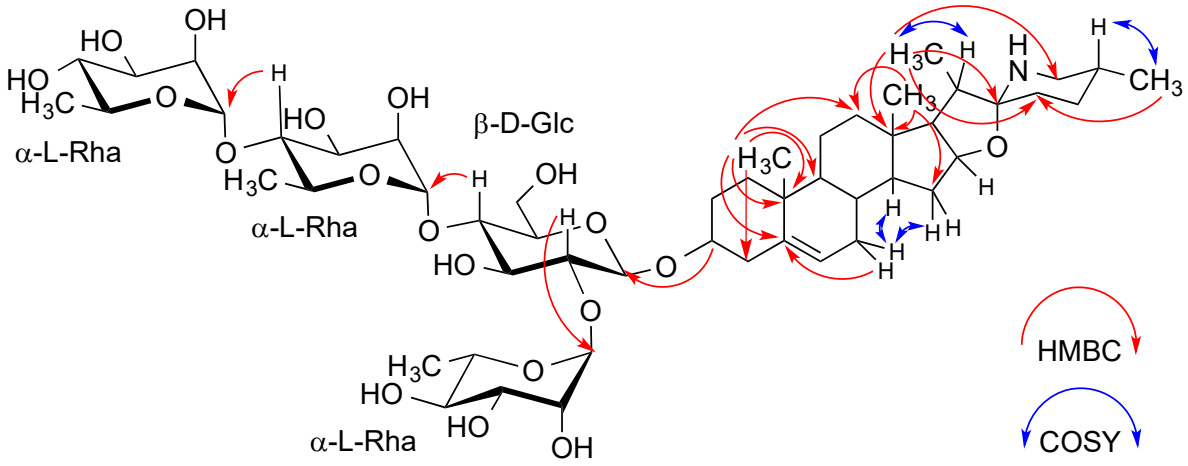

Figure 3. Key HMBC and ^{1}H-^{1}H COSY correlations observed in SGA **1**.

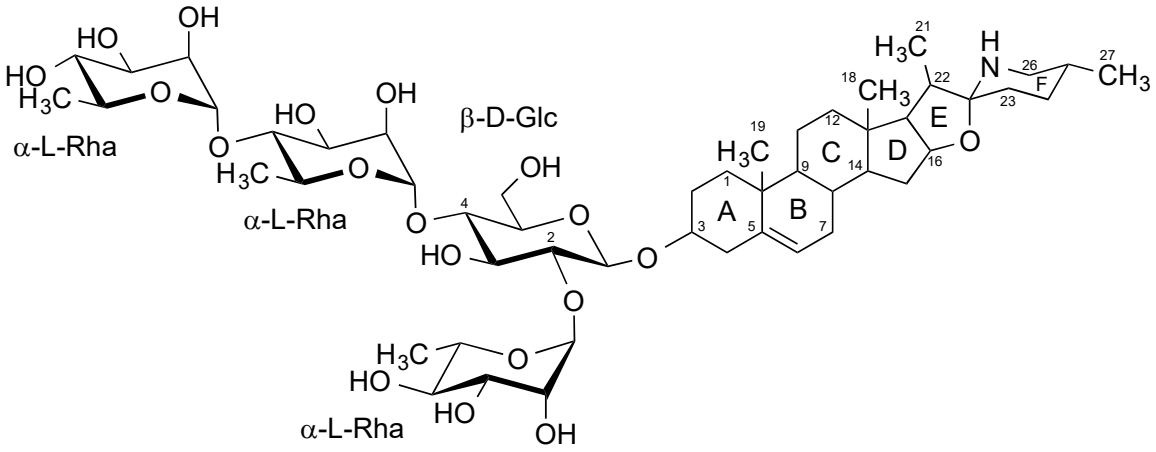

Figure 4. Structure of the new SGA **1**.

SGA **1** (Figure 4) identified in this study possesses the aglycone solasodine and four sugar moieties, namely three rhamnopyranose residues and a galactopyranose moiety attached at the 3-OH position of the aglycone. It was evaluated for its cytotoxic potential and mechanism of action. The activity of **1** was, for SAR discussions, compared to that of seven structurally related SAGs, namely solasodine, α-solasonine, β-solamargine, khasianine, β-solamarine, α-solanine and tomatidine HCl (Figure 5) that were also evaluated for their cytotoxic activity and mechanism.

In our study α-solasodine showed no cytotoxic activity against any of the cell lines tested. Similarly α- solasodine was inactive against MCF-7 and other cell lines tested in a previous study and only showed detectable activity against prostate cancer (PC3) cells (13.6 µM) (15). In contrast, tomatidine HCl, which was also inactive against all cell lines tested in our study, inhibited growth of human mammary cancer cells, BCAP, in a previous study (27).

A number of studies have reported that SGAs are more cytotoxic than their respective aglycones alone (17, 28). Our study confirmed this by showing no detectable cytotoxic activity for the aglycone α–solasodine, but the same aglycone with three sugars attached, namely α-solasonine (Gal, Rha and Glc in a branched arrangement) showed potent selective cytotoxicity.

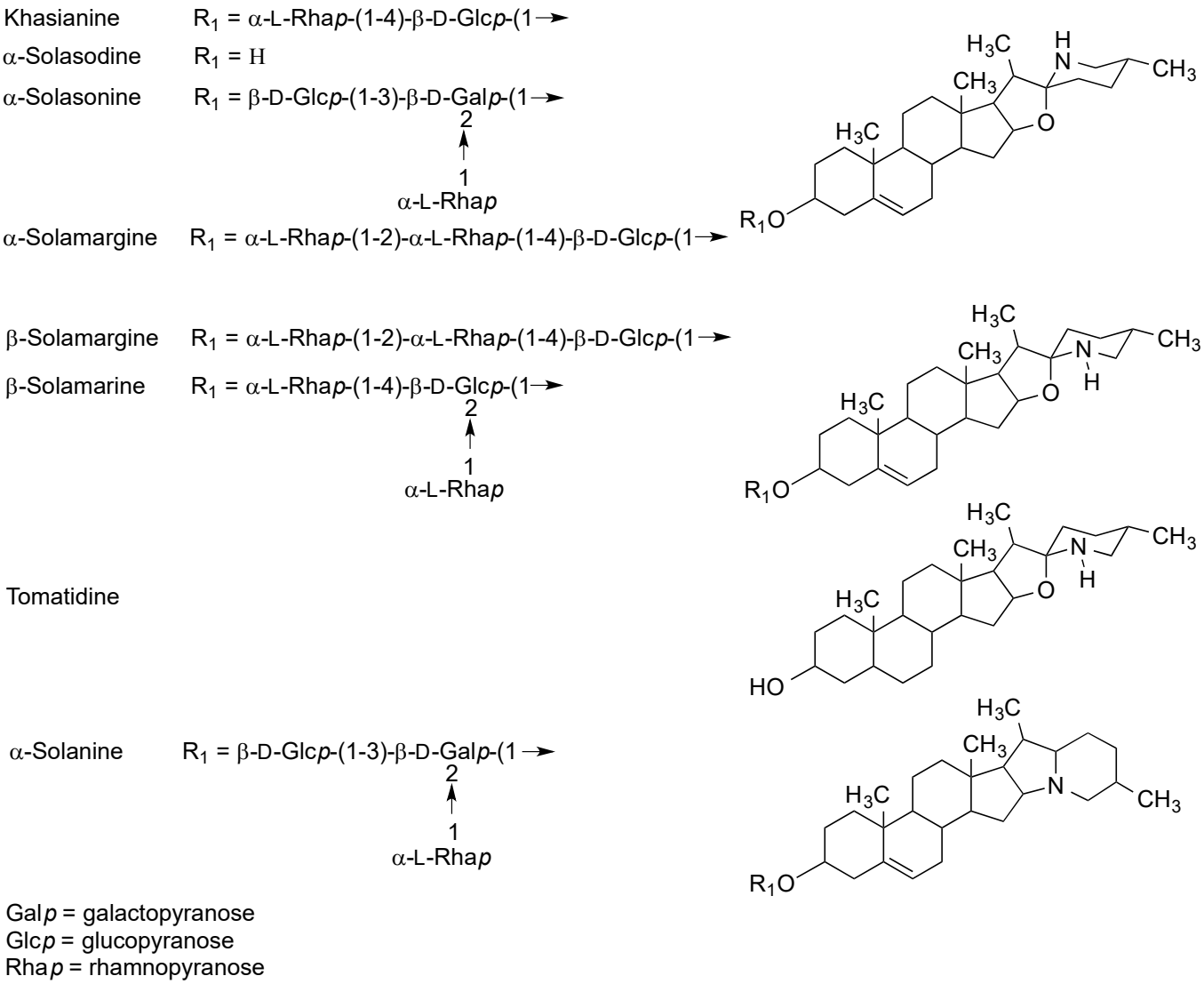

Figure 5. Structures of selected SGA analogues.

Previous studies have found that the type, number, as well as order of the sugar residues attached to the aglycone have a significant influence on the cytotoxic activity of SGAs (14,17), and our data support this. In our study khasianine, where the glycone is comprised of two sugar moieties (α-L-Rha-(1-4)-β-D-Glc-(1-aglycone), only showed detectable activity against MCF-7 cells (IC_{50} of 19.89 μM). However, SGA **1** with the same aglycone as khasianine , but with four sugars, two additional sugars to the khasianine arrangement (one added to the C4 of the α-L-Rha of khasianine, the other, α-L-Rha, attached to C2 of the -β-D-Glc of khasianine), showed significant toxicity to all cell lines tested (e.g. MCF-7 IC_{50} of 2.62 μM).

Our study also indicates that the type of aglycone does not impact significantly on the cytotoxic activity overall if the sugar moieties are being kept the same. For example, a comparison of α-solanine and α-solasonine, where the glycone contains the exact same sugars and arrangement, but the aglycone is variant in rings E and F (see Figure 5) indicates that a variation of the aglycone does not lead to significant changes in the selectivity of cytotoxicity. The cytotoxic activity of α-solasonine and α-solanine on MCF-7 and MDA-MB-231 cells was similar (IC_{50} values: 5.09 vs 4.57 and 8.36 vs 6.94 μM). In our study both compounds showed greater cytotoxicity against MCF-7 cells than previously reported (IC_{50} values of 10.97 μM and 25.44 μM, respectively) (29). We also tested β-

solamargine for which no cytotoxic activity data exists, and determined an IC_{50} of 5.01 μM against estrogen-dependent breast cancer cells (MCF-7). This value is similar to the cytotoxic activity reported for α-solamargine against MCF-7 (IC_{50} values reported: 2.1 μM (30), 2.5 μM (17) and 8.2 μM (15, 31). Thus, the structural difference between β-solamargine and α-solamargine (being a β-solasodine *vs* α-solasodine aglycone, sugar moieties are identical, see Figure 5) does not seem to significantly influence the cytotoxicity of the compounds.

Moreover, β-solamargine with one Rha more than khasianine and one less that SGA **1** exhibited a very similar cytotoxicity profile to that of SGA **1**. This suggests that cytotoxicity is notably enhanced with the addition of the second Rha to the linear chain (Rha-Rha-Glc-aglycone) and that the addition of the third Rha (SGA **1**, joined to the Glc (Rha-Rha-Glc(Rha)-aglycone) does little to further enhance this activity. Therefore this demonstrates the importance of the two terminal α-L-Rha sugars on SGA **1** and the significant increase in cytotoxicity as a consequence of these being present (see Table 2 and Figure 5).

Apoptosis plays a central role in the development and homeostasis of multicellular organisms to eliminate unwanted cells. Induction of apoptosis of cancer cells plays crucial roles in the anticancer activity of many anticancer agents (24). To determine whether the SGA **1** induces apoptosis, we conducted a 24 h apoptosis assay on SGA **1** and other known cytotoxic SGAs against MCF-7 cells at their IC_{50} concentrations.

In this study, SGA **1** showed the highest apoptotic (AV^+/PI^-) effect (32%) among all the SGAs tested. The impact of the number of sugar moieties and type of linkage on cytotoxic and apoptosis activity of SGAs against various cancer cell lines has previously been reported (14, 32). For example, α-solamargine was shown to be 4 times more apoptotic than khasianine, most likely due to the presence of an additional Rha moiety (27). SGA **1** seems to be similar in its cytotoxicity and apoptotic potential to β-solamarine and β-solamargine, respectively, compounds with very similar sugar moiety arrangements and with only a slightly different aglycone to SGA **1** (different distal stereo-centre on the aglycone at the linkage of rings E and F, which defines it as an α or β-configuration).

That α-solanine induces apoptosis has been reported using human hepatoma cells (33). For α-solamargine reports exist on apoptosis-inducing potential and enhancement of susceptibility to the anticancer drugs trastuzumab and epirubicin on MCF-7 and other breast cancer cells (SK-BR-3) (34), as well as on colon, gastric, liver, lung and other cell types (17, 35). However, to our knowledge the apoptotic potential of β-solamargine, β-solamarine and α-solasonine has not previously been reported.

We also further evaluated the effect of the new SGA **1** on the MCF-7 cell cycle using PI staining. Treatment with SGA **1** lead to a slight, but significant, accumulation of cells in the G1 phase (15.7% increase of cells in comparison to untreated cells). A similar effect on the MCF-7 cell cycle was observed following treatment with β-solamargine, β-solamarine and α-solasonine, although the effect observed for SGA **1** was slightly more pronounced.

A clear SAR analysis is difficult given that SGA **1**, β-solamargine, β-solamarine and α-solasonine arrest cells in G1 to a similar extent. However, the slightly more pronounced effect of SGA **1** could be due to the presence of a larger number of sugar residues (Figures 1 and 5). Importantly, this study provides the first report of the effect of β-solamargine, β-solamarine, and α-solasonine on the cell cycle. Only α-solamargine has been investigated previously, showing an arrest of lung cancer cells (H441, H520, H661 and H69) in their sub-G1 phase (35). Moreover, in contrast to the other SGAs tested, here we saw a significant increase in the percentage of MCF-7 cells arrested in the S-phase for α-solanine, which correlates with reports in the literature (29). Our study also found that paclitaxel induced G2/M cell cycle arrest, a result that is supported by another cell cycle study previously performed on MCF-7 with paclitaxel for 48 h (36).

In conclusion, the results of this study confirm that some SGAs have significant cytotoxic activity, with the new SGA **1** and β-solamarine being the most cytotoxic SGAs overall. The study also highlights the importance of sugar moieties for the cytotoxic activity of SGAs and shows for the first time apoptotic and cell cycle effects for β-solamargine, β-solamarine and α-solasonine.

The potent cytotoxic activity of the new SGA **1** against MCF-7 cells can be attributed to its ability to induce apoptosis, an effect that seems to be due to its ability to arrest cells in the G1 phase. The

arrest of cells is G1 phase suggests a decrease in the expression of proteins (e.g., cyclin D1 and CDK-4) that regulate the G1/S checkpoint. Cells that do not clear this checkpoint do not pass through to the S phase, instead entering the dormant G_0 phase in which there is no growth or division.

Further studies investigating for example caspase activity, expression of Bcl-2 and Bcl-xL and the regulation of HER2/neu will be required to further clarify the exact mechanism by which SGA **1** inhibits the growth of MCF-7 cells. However, our study already highlights the great potential of SGA **1** as an anticancer agent.

ACKNOWLEDGEMENT

The authors wish to acknowledge Nadia X. Arndt for her assistance with flow cytometry experiments. R.A. was funded by a Griffith University Postgraduate Research Scholarship (GUPRS) and a Griffith University International Postgraduate Research Scholarship (GUIPRS).

CONFLICT OF INTEREST

The authors have declared that there is no conflict of interest.

REFERENCES

1. Ghani A. Medicinal plants of Bangladesh with Chemical Constituents and Uses. Dhaka, Bangladesh.: Asiatic Society of Bangladesh; 2003.
2. Agarwal R, Singh R, Siddiqui IR, Singh J. Triterpenoid and prenylated phenol glycosides from *Blumea lacera*. Phytochemistry, 38(4):935-938, 1995.
3. Ragasa CY, Wong J, Rideout JA. Monoterpene glycoside and flavonoids from *Blumea lacera*. J Nat Med, 61(4):474-475, 2007.
4. Singh UP, Parthasarathy R. Comparative antidiarrhoel activity of ethanolic extract of root of *Blumea lacera* var lacera and Blumea eriantha DC on experimental animals. J Pharm Biomed Sci, (17):16, 2012.
5. Chiang L-C, Cheng H-Y, Chen C-C, Lin C-C. *In vitro* anti-leukemic and antiviral activities of traditionally used medicinal plants in Taiwan. Am J Chin Med, 32(5):695-704, 2004.
6. Uddin Shaikh J, Grice ID, Tiralongo E. Cytotoxic effects of Bangladeshi medicinal plant extracts. Evid Based Complement Alternat Med, 2011:578092, 2011.
7. Rao CB, Rao TN, Muralikrishna B. Flavonoids from *Blumea lacera*. Planta Med, 31(3):235-237, 1977.
8. Iyer GN, Sane RT, Menon S. Mosquito repellent essential oil from *Blumea lacera*. In. Application: US: (India). 2004. p. 12 pp.
9. Bohlmann F, Zdero C. Coniferyl alcohol derivative from *Blumea lacera*. Tetrahedron Lett, (2):69-70, 1969.
10. Le VH, Tran TM, Nguyen XD. Essential oils of *Blumea lacera* (Burm.F) DC .(Asteraceae) produced from aerial parts of plants grown in central Vietnam. J Essent Oil-Bear Plants, 6(1):36-40, 2003.
11. Laakso I, Seppanen-Laakso T, Hiltunen R, Ekundayo O. Composition of the essential oil of *Blumea lacera* DC. (Asteraceae) leaves from Nigeria. Flavour Fragrance J, 4(2):73-75, 1989.
12. Baslas KK, Deshapande SS. Essential oil from the leaves of *Blumea lacera*. J Indian Chem Soc, 27:25-28, 1950.
13. Pal R, Moitra SK, Chakravarti NN, Adhya RN. Campesterol from *Blumea lacera*. Phytochemistry, 11(5):1855, 1972.
14. Li S-y, He D-j, Zhang X, Ni W-h, Zhou Y-f, Zhang L-p. Modification of sugar chains in glycoalkaloids and variation of anticancer activity. Chem Res Chin Univ, 23(3):303-309, 2007.
15. Cui CZ, Wen XS, Cui M, Gao J. Sun B, Lou HX. Synthesis of solasodine glycoside derivatives and evaluation of their cytotoxic effects on human cancer cells. Drug Discoveries & Therapeutics 6(1):9-17, 2012.
16. Chang L-C, et al. The rhamnose moiety of solamargine plays a crucial role in triggering cell death by apoptosis. Biochem Biophys Res Commun, 242:21-25, 1998.
17. Nakamura T, Komori C, Lee Y-y, Hashimoto F, Yahara S, Nohara T, Ejima A. Cytotoxic activities of Solanum steroidal glycosides. Biol Pharm Bull, 19(4):564-566, 1996.
18. Ono M, Takamura C, Sugita F, Masuoka C, Yoshimitsu H, Ikeda T, Nohara T. Two new steroid glycosides and a new sesquiterpenoid glycoside from the underground parts of *Trillium kamtschaticum*. Chem Pharm Bull, 55(4):551-556, 2007.
19. Yoshikawa M, Xu F, Morikawa T, Pongpiriyadacha Y, Nakamura S, Asao Y, Kumahara A, Matsuda H. Medicinal flowers. XII. New spirostane-type steroid saponins with antidiabetogenic activity from *Borassus flabellifer*. Chem Pharm Bull, 55(2):308-316, 2007.
20. Lorey S, Porzel A, Ripperger H. Steroid alkaloid glycosides from *Solanum coccineum*. Phytochemistry, 41(6):1633-1635, 1996.
21. Mahato SB, Sahu NP, Ganguly AN, Kasai R, Tanaka O. Steroidal alkaloids from *Solanum khasianum*: application of carbon-13 NMR

spectroscopy to their structural elucidation. Phytochemistry, 19(9):2017-2020, 1980.
22. Milner SE, et al. Bioactivities of glycoalkaloids and their aglycones from Solanum species. J Agric Food Chem, 59:3454-3484, 2011.
23. Patel K, Singh RB, Patel DK. Medicinal significance, pharmacological activities, and analytical aspects of solasodine: A concise report of current scientific literature. Journal of Acute Disease:92-98, 2013.
24. Wang Y, Zhang Y, Zhu Z, Zhu S, Li Y, Li M, Yu B. Exploration of the correlation between the structure, hemolytic activity, and cytotoxicity of steroid saponins. Bioorg Med Chem, 15(7):2528-2532, 2007.
25. Man S-L, Gao W-Y, Zhang Y-J, Huang L-Q, Liu C-X. Chemical study and medical application of saponins as anti-cancer agents. Fitoterapia, 81(7):703-714, 2010.
26. Gao J, Li X, Gu G, Sun B, Cui M, Ji M, Lou H-X. Efficient synthesis of trisaccharide saponins and their tumor cell killing effects through oncotic necrosis. Bioorg Med Chem Lett, 21(2):622-627, 2011.
27. Yang X, Wang R, Ran F, Sun S. Inhibitory effects of 26 alkaloids compounds against growth of human mammary cancer cell line BCAP *in vitro*. Zhongguo Xiandai Zhongyao 9(3): 9-11, 2007.
28. Esteves-Souza A, Sarmento da Silva TM, Alves CCF, de Carvalho MG, Braz-Filho R, Echevarria A. Cytotoxic activities against Ehrlich carcinoma and human K562 leukemia of alkaloids and flavonoid from two solanum species. J Braz Chem Soc, 13(6):838-842, 2002.
29. Ji Y, Liu J, Gao S. Effects of solanine on microtubule system of human breast cancer MCF-7 cells. Zhongcaoyao, 43(1):111-114, 2012
30. Wei G, et al. Total synthesis of solamargine. Bioorganic & Medicinal Chemistry Letters 21(10):2930-2933, 2011.
31. Sun L, Zhao Y, Yuan H, Li X, Cheng A, Lou H. Solamargine, a steroidal alkaloid glycoside, induces oncosis in human K562 leukemia and squamous cell carcinoma KB cells. Cancer Chemotherapy and Pharmacology, 67(4):813-821, 2011.
32. Chang L-C, Tsai T-R, Wang J-J, Lin C-N, Kuo K-W. The rhamnose moiety of solamargine plays a crucial role in triggering cell death by apoptosis. Biochemical and Biophysical Research Communications, 242(1):21-25, 1998.
33. Gao S, Zou X, Ji C, Wang H. Study of solanine on apoptosis in HepG2 cell. Harbin Shangye Daxue Xuebao, Ziran Kexueban, 23(6):644-650, 2007.
34. Shiu LY, Liang CH, Chang LC, Sheu HM, Tsai EM, Kuo KW. Solamargine induces apoptosis and enhances susceptibility to trastuzumab and epirubicin in breast cancer cells with low or high expression levels of HER2/neu. Bioscience Reports, 29(1):35-45, 2009.
35. Liu L-F, Liang C-H, Shiu L-Y, Lin W-L, Lin C-C, Kuo K-W. Action of solamargine on human lung cancer cells - enhancement of the susceptibility of cancer cells to TNFs. FEBS Lett, 577(1-2):67-74, 2004.
36. Saunders DE, Lawrence WD, Christensen C, Wappler NL, Ruan H, Deppe G. Paclitaxel-induced apoptosis in MCF-7 breast-cancer cells. International Journal of Cancer, 70(2):214-220, 1997.

Appendix A: Supplementary data

Contents

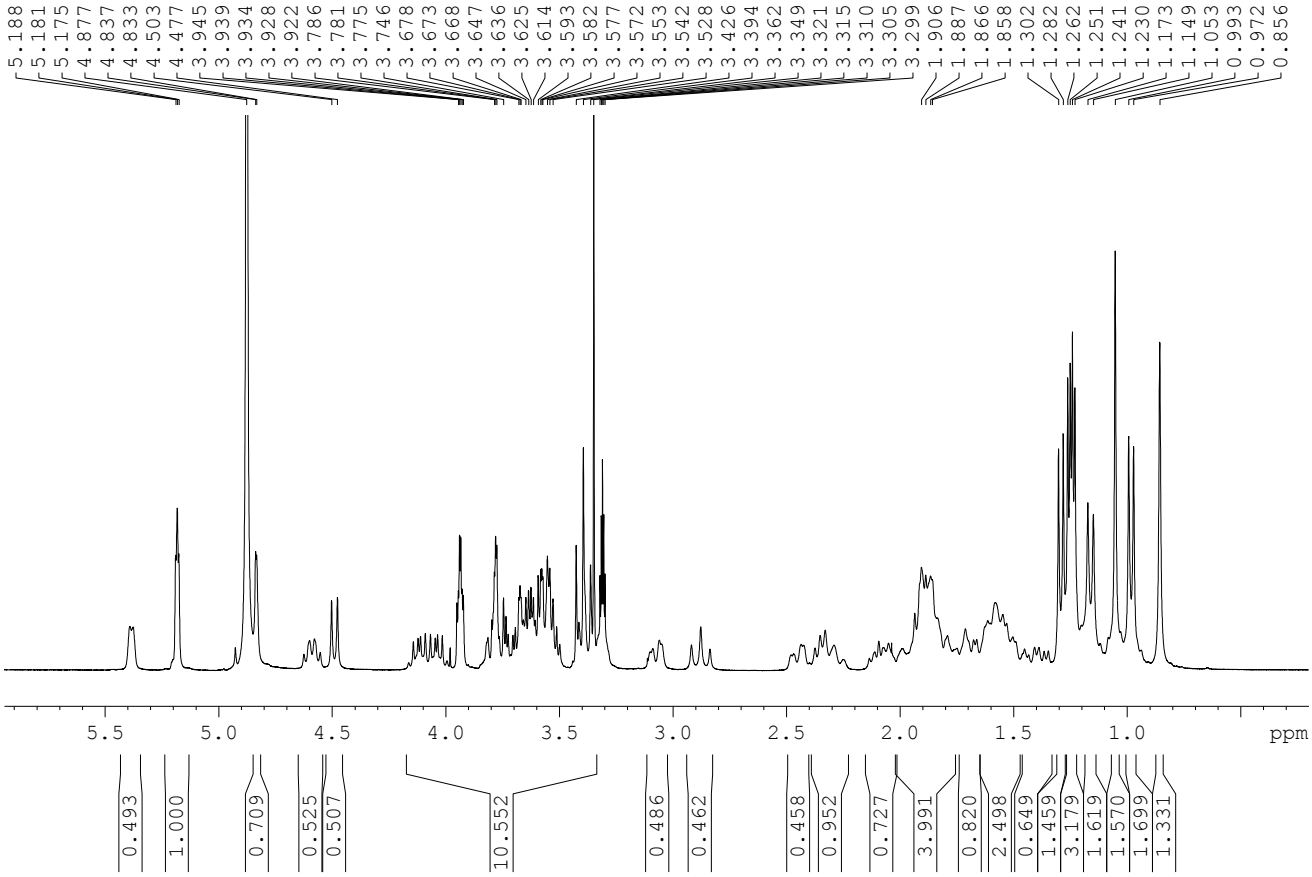

Figure S1. ^{1}H NMR (600 MHz, CD_3OD) spectrum of SGA **1** (CD_3OD at 300 MHz).

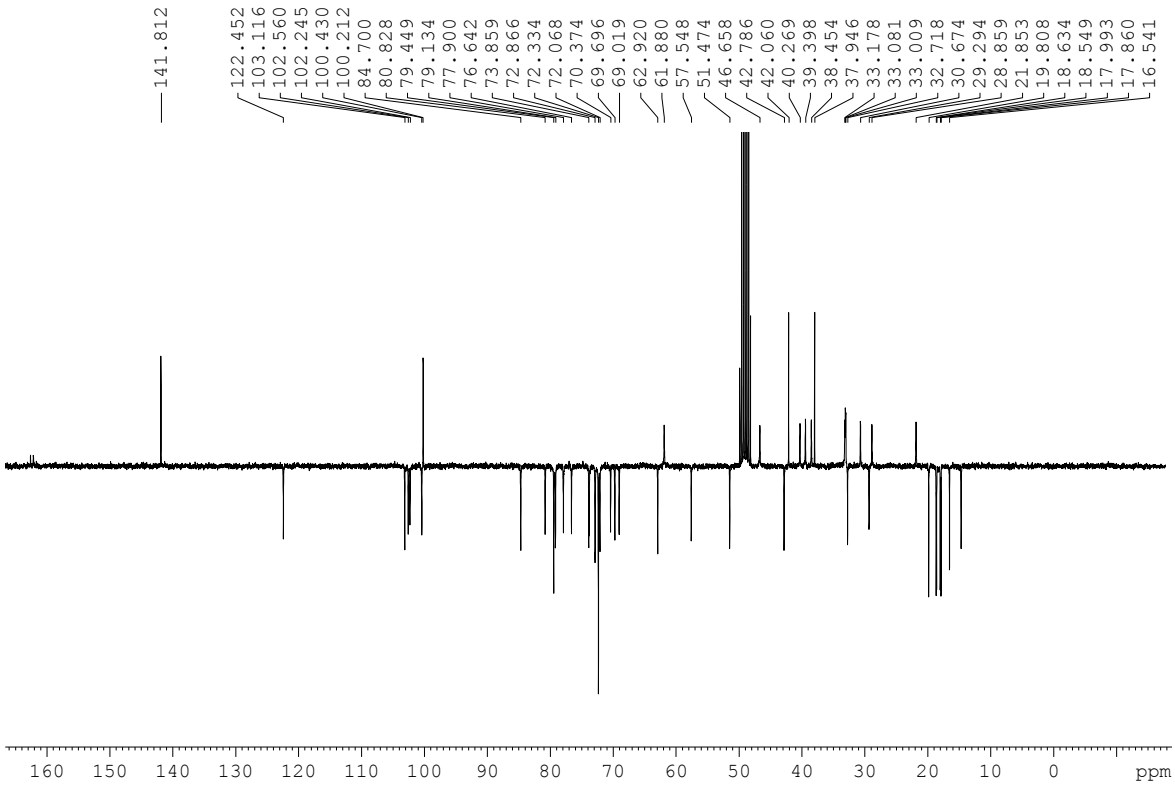

Figure S2. ^{13}C NMR (Jmod, CD_3OD at 75 MHz) spectrum of the new SGA **1**.

Graphs of cytotoxicity tests of SGA 1 and the selected SGA analogues

A total of eight SGAs including the new SGA **1** have been tested for their cytotoxic activity against different cancer as well as healthy cell lines at different concentrations. All SGAs showed concentration dependent cytotoxicity (Figures S3-S10).

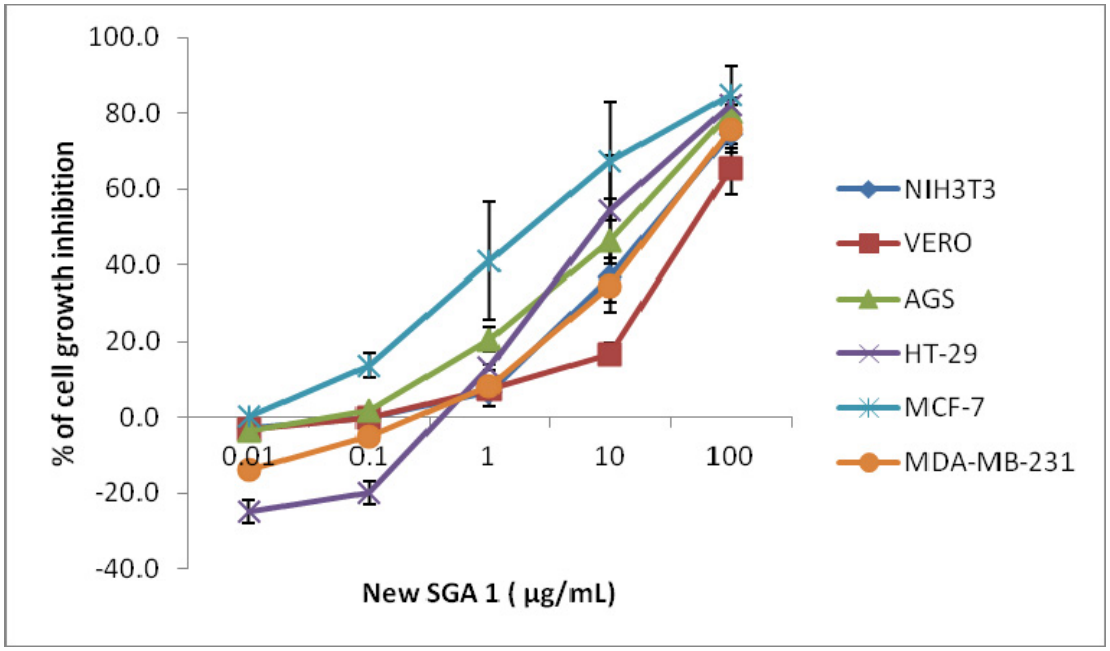

Figure S3. Percent (%) of cell growth inhibition of SGA **1** against the tested cell lines.

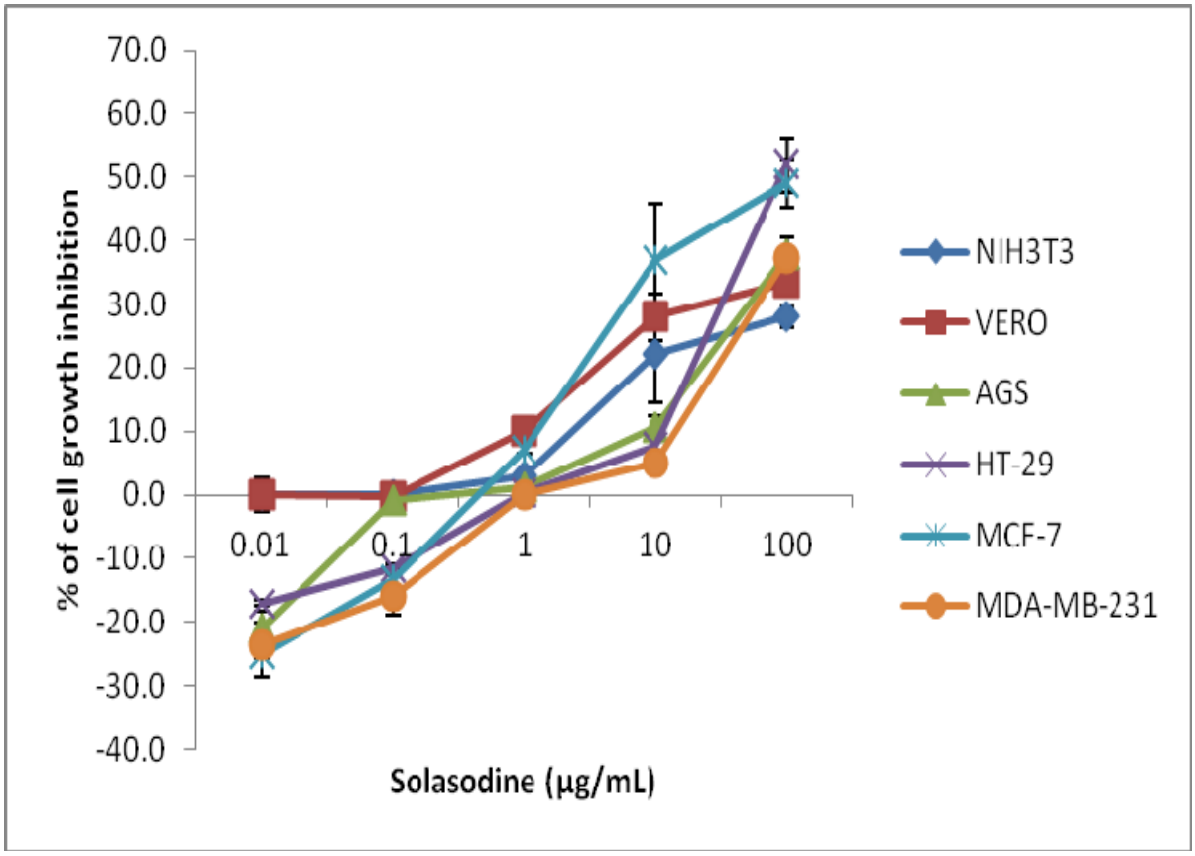

Figure S4. Percent (%) of cell growth inhibition of α-solasodine against the tested cell lines.

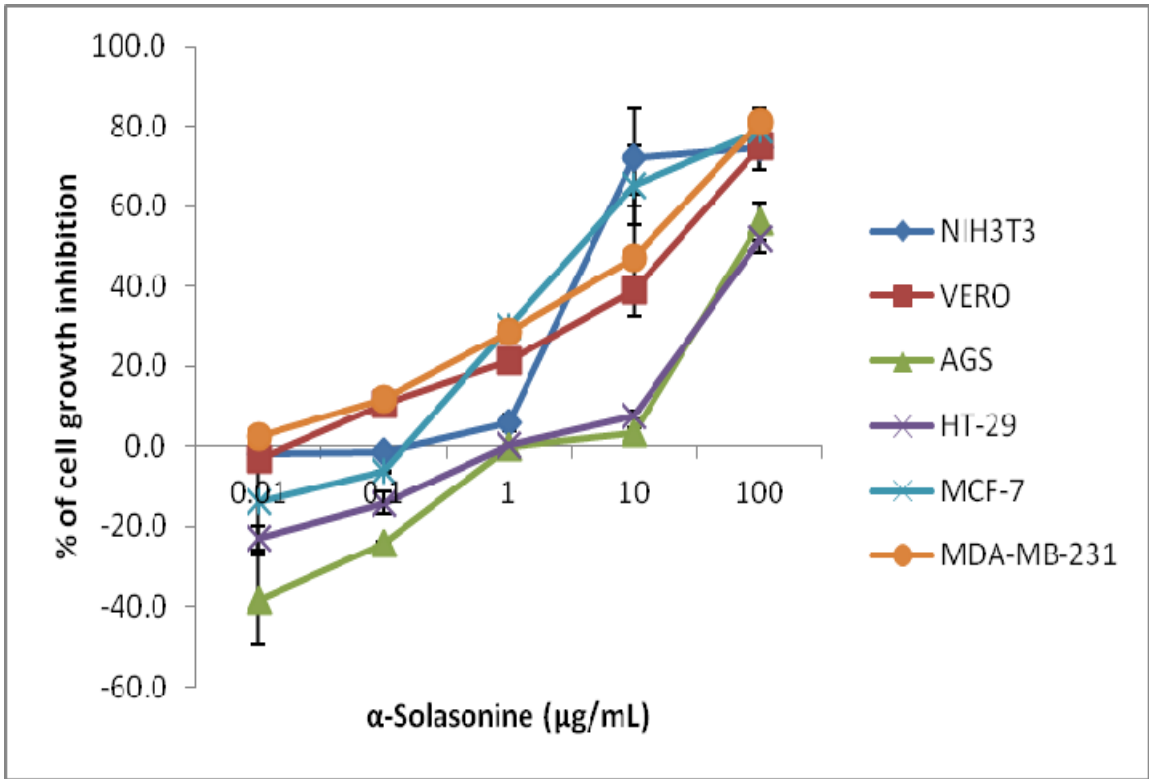

Figure S5. Percent (%) of cell growth inhibition of SGA α-solasonine against the tested cell lines.

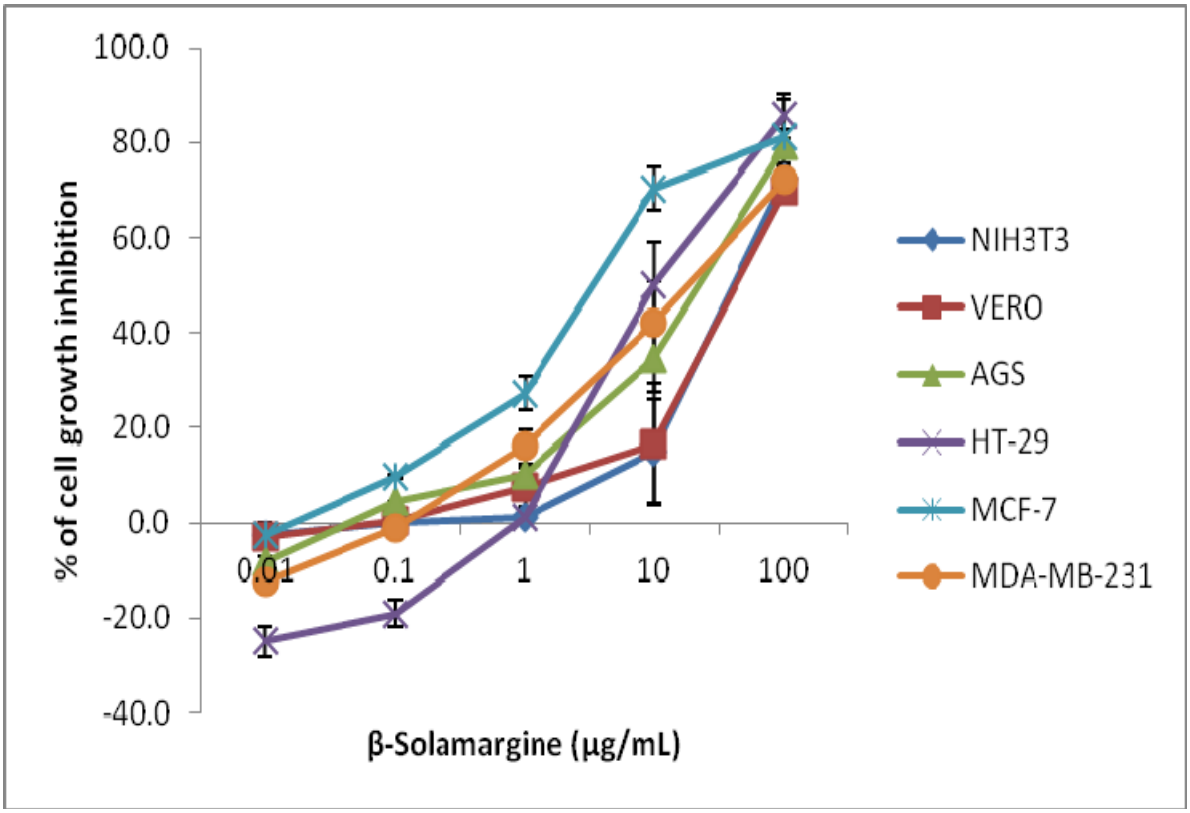

Figure S6. Percent (%) of cell growth inhibition of SGA β-solamargine against the tested cell lines.

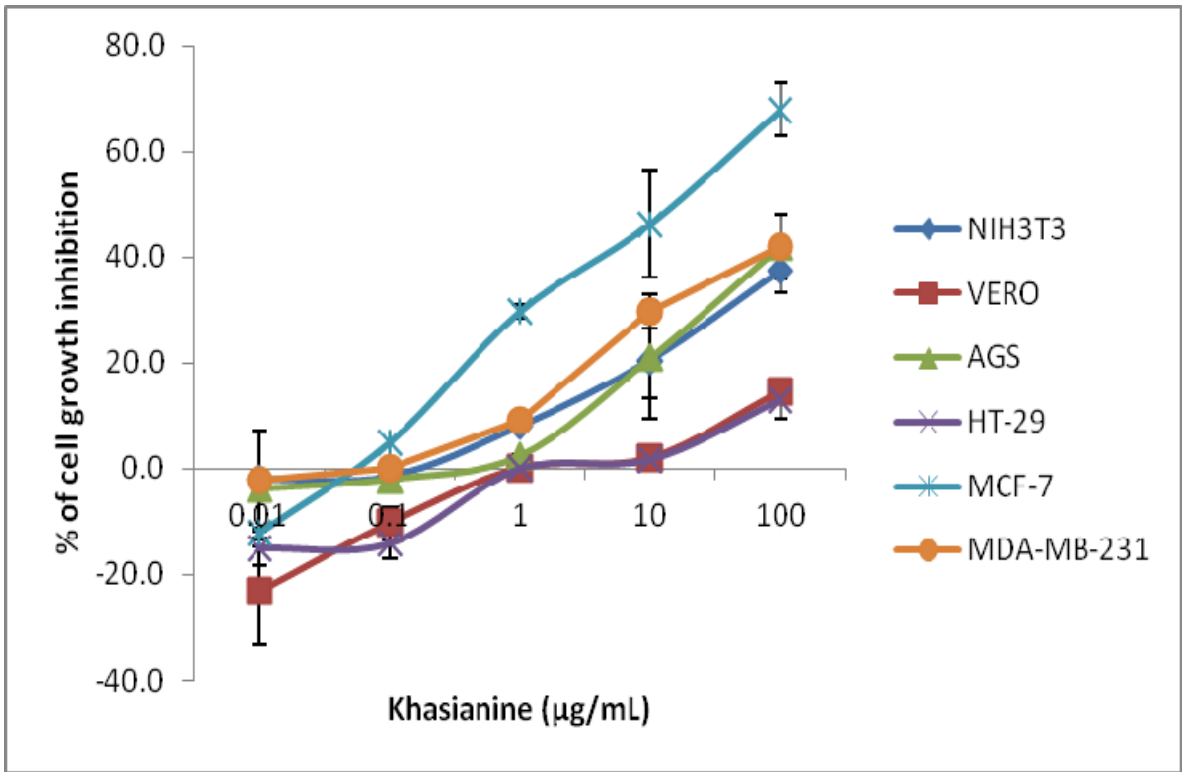

Figure S7. Percent (%) of cell growth inhibition of SGA khasianine against the tested cell lines.

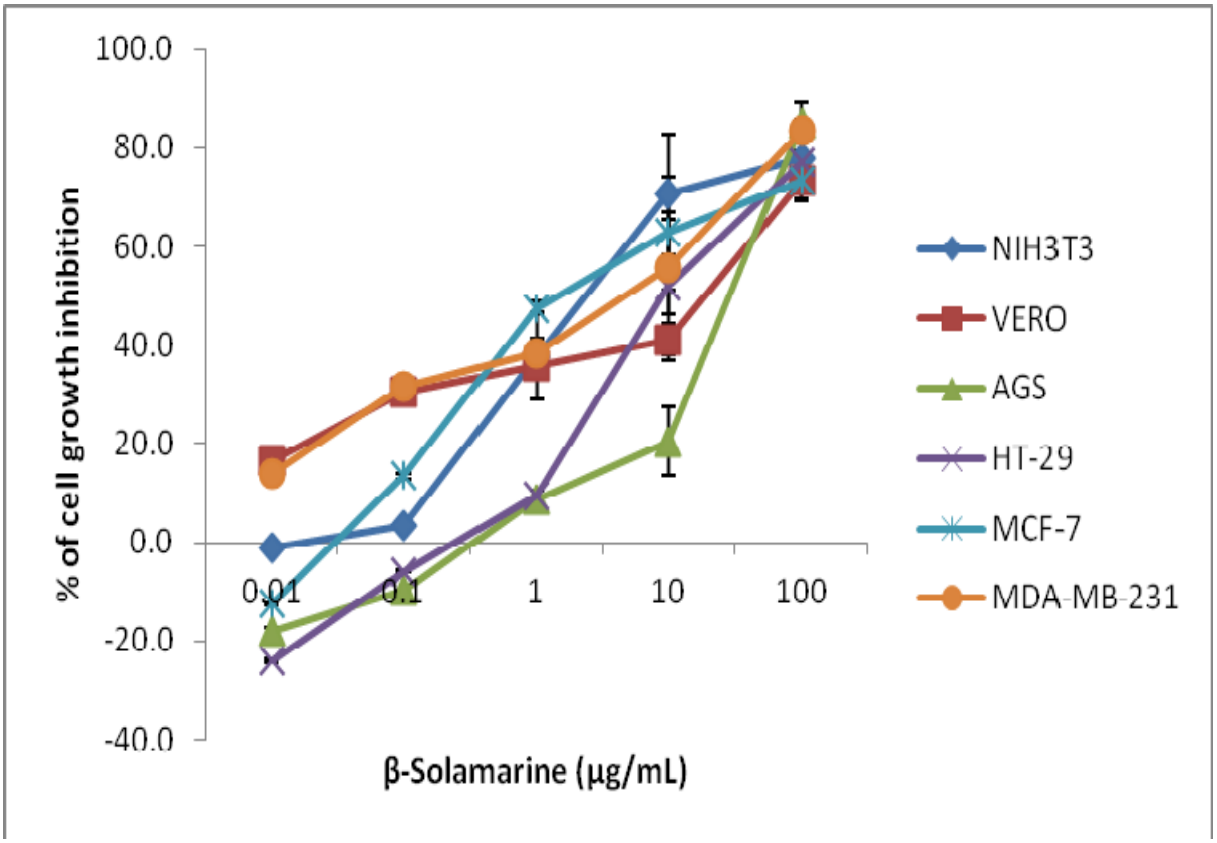

Figure S8. Percent (%) of cell growth inhibition of SGA β-solamarine against the tested cell lines.

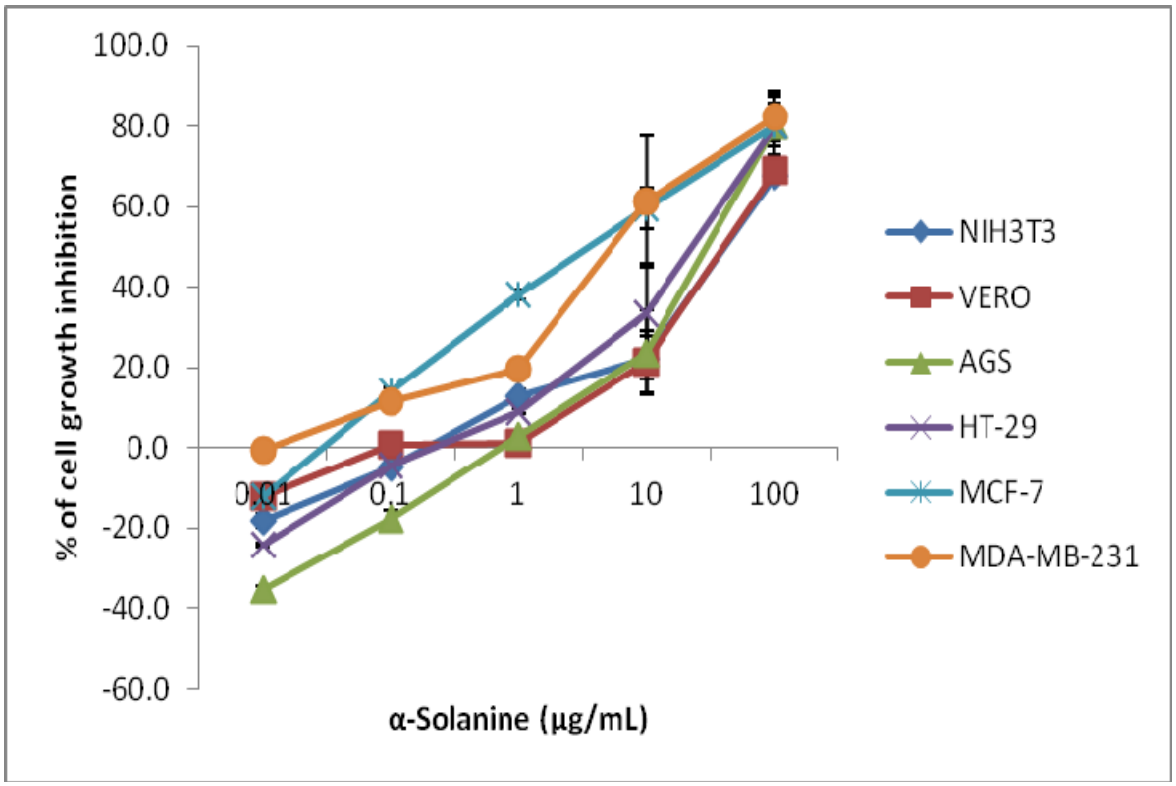

Figure S9. Percent (%) of cell growth inhibition of SGA α-solanine against the tested cell lines.

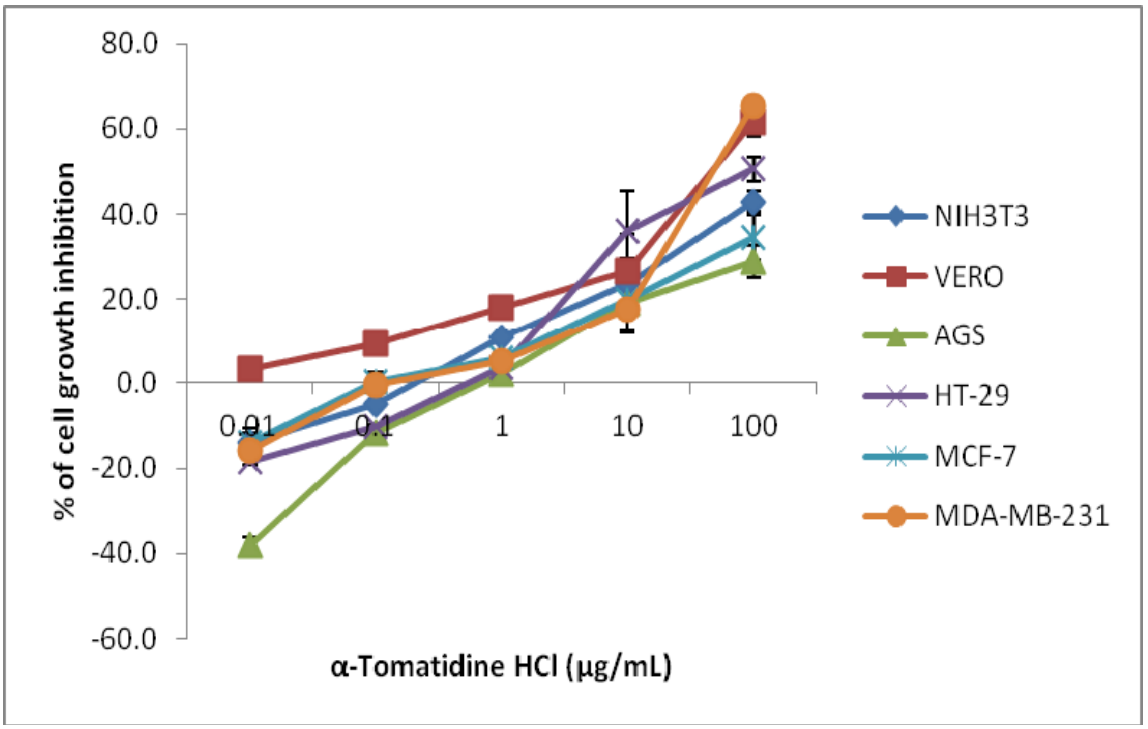

Figure S10. Percent (%) of cell growth inhibition of tomatidine HCl against the tested cell lines.